VOL. 13, NO. 24, DECEMBER 2018 ISSN 1819-6608
ARPN Journal of Engineering and Applied Sciences

www.arpnjournals.com

DEVELOPMENT OF A REAL-TIME MICROCOMPUTER-BASED DATA ACQUISITION SYSTEM FOR A VERY LOW FREQUENCY (VLF) MONITOR FOR SPACE WEATHER STUDIES

April Jem H. Saccuan[1], Reynalin B. Deveza[1], Shawn Michael L. Lamod[1], Jocelyn F. Villaverde[1] and Ernest P. Macalalad[2]
[1]School of Electrical, Electronics, and Computer Engineering, Mapúa University, Manila, Philippines
[2]Department of Physics, Mapúa University, Manila, Philippines
E-Mail: epmacalalad@mapua.edu.ph

ABSTRACT

Ionosphere is the region in the atmosphere where ionization takes place. Its structure varies by altitude, time, and other solar or cosmic activities that affect the propagation of radio signals. Variations in the signal strengths of very low frequency signals as a result of ionospheric changes is a way to measure changes and disturbances in the ionosphere. Stanford University developed a VLF based monitor called SuperSID for monitoring changes within the ionosphere. In this project, an enhanced version of the SuperSID software was introduced, which includes a real-time visualization of signal strength versus time plot for the current day; and a plot function for a quiet day curve. The constructed microcomputer-based data acquisition system was validated using another SuperSID monitor from Stanford. Both are stationed in Manila, Philippines and are configured to monitor NWC (19.8 kHz) and NDT (22.2 kHz) transmitters. A statistical test was performed to validate the association between the monitors and resulted with an average correlation coefficient of 0.958 and 0.948 for NWC and NDT transmitters. Also, a successful characterization of solar flare and thunderstorm was done using an enhancement algorithm.

Keywords: VLF, microcomputer, Super SID monitor, space weather, ionosphere.

INTRODUCTION

Space weather is a branch of science that is concerned with the conditions in the solar terrestrial environment which consists of the upper part of the Earth's atmosphere, the outer part of the Earth's magnetosphere and solar emissions such as radiation and matter that affect them. Solar radiation as it reaches gas or other molecules in the Earth's upper atmosphere, free its electrons thereby ionizing them. The region in the atmosphere wherein sufficient ionization takes place that can affect the propagation of radio signals is called the ionosphere. The structure of the ionosphere varies greatly with altitude (e.g. ionospheric layers), time (e.g. seasonal changes, and day-night cycles), geographic location (e.g. poles, geomagnetic equatorial regions), and solar activity [1].

Instruments that monitor the ionosphere include: Ionosondes, Global Navigation Satellite System (GNSS) and GNU Radio Broadcasting Beacon (GRBR). An ionosonde is an instrument that makes use of High Frequency (HF) signals to measure the virtual height of the ionosphere [2]. GNSS makes use of L-band signals while GRBR is a legacy of the GNSS systems that usesultra-high frequency (UHF) and very high frequency (VHF) signals [3], [4]. Another method of monitoring is by making use of very low frequency (VLF) radio signals. VLF signals from ground transmitters are "bounce" back to the Earth due to their large wavelengths. This property of VLF signals became the basis for long distance radio communication without using an Earth orbiting satellite. Stanford University developed a VLF based monitor called SuperSID that can monitor changes within the ionosphere caused by sudden ionospheric disturbances (SID) [5]. The ionosphere due to its ionization affects the propagation of radio signals. Pronounced changes in the signal strengths of VLF signals due to ionospheric changes had made it viable to measure changes and disturbances in the ionosphere.

Although there are existing Stanford's SuperSID monitors around the globe, SID data, or the seismograph-like data where VLF relative signal strengths are tracked over time, data plotting is not immediate (i.e. non-real-time). It was discussed previously that not only altitude, diurnal effects and solar activity affect the structure of the ionosphere but also by geographic location. References [6]-[8] discussed that the atmosphere is more ionized in an event of SID due to solar flares, coronal mass ejections and other cosmic events within the geomagnetic equator (where the Philippines is located) [7]-[9]. However, known locations of SuperSID monitors within the region is scarce. Additionally, the SuperSID program requires a desktop computer or laptop to run which takes up more space is susceptible to RF noise that can obscure data [10], [11], and generally is more resource intensive to setup and maintain.

This study generally aims to develop a real-time microcomputer-based data acquisition system for a very low frequency monitor for space weather studies. Specifically, this study aims: (1) to construct and install a loop antenna to detect VLF signals, and a preamplifier to boost the signal which is to be converted from analog to digital; (2) to develop a software for real-time visualization of VLF signal strength, and; (3) to compare the acquired data during quiet days with disturbed days when there are ionospheric and space weather events.

The study of monitoring the strength of received radio signals from distant VLF transmitters as they bounce from the ionosphere have major importance to communications (radio and satellite) and navigation (GNSS) as detection of disruptions brought by SIDs are immediate. In a real-time monitoring device, sudden changes in the ionosphere can be immediately given to various agencies related to space weather research and application such as the Department of Science and Technology of the Philippines which operates the country's first low Earth orbiting (LEO) micro-satellite DIWATA-1 and MAYA-1. Changes in the ionospheric electron density can affect LEO satellite's trajectory, due to satellites experiencing orbital decay and atmospheric drag [12]. In events of possible severe disturbances in the ionosphere, telecommunications personnel can be informed and identify the source of the problem as a natural event rather than equipment failure. The use of a microcomputer in this research simplifies component, space and power requirements in configuring a data acquisition system compared to a full desktop setup. Finally, the data can be contributed to the VLF world data repository hosted at Stanford University, for future space weather studies and for complementing the measurements of other ionospheric monitoring devices.

This research only measured VLF signal strength patterns that could identify the occurrence of SIDs, particularly of solar flares and thunderstorms, as described by their trends or "signatures". In addition, the date and time the disturbances happened and the number of peak points for flares were also reported. Monitoring of VLF signal strengths of selected frequencies at five second intervals, 24 hours per day for thirty (30) days was carried out. The analysis of SIDs caused by solar flares is limited in the local daytime part of each day as it would be unobservable otherwise. The study did not cover the determination of the changes in the structure of the ionosphere with respect to time, including the amount of ionospheric density, total electron content, nor the identification of where ionospheric disturbances originated. It also did not cover correcting any disruptions in communication and navigation nor forecast space weather.

METHODOLOGY

Figure-1 shows the over-all flow of track implemented in this research. The construction of the loop antenna and preamplifier for the VLF monitoring system is under the hardware development, which also includes the gathering of materials and its assembly. Software development tackles the overview of the Raspberry Pi Configuration and the development of the MIT-PH2 SuperSID Software. Proceeding with the testing, the developed software was integrated with the hardware according to the research setup. Finally, the acquired data from this study were plotted for analysis and verification.

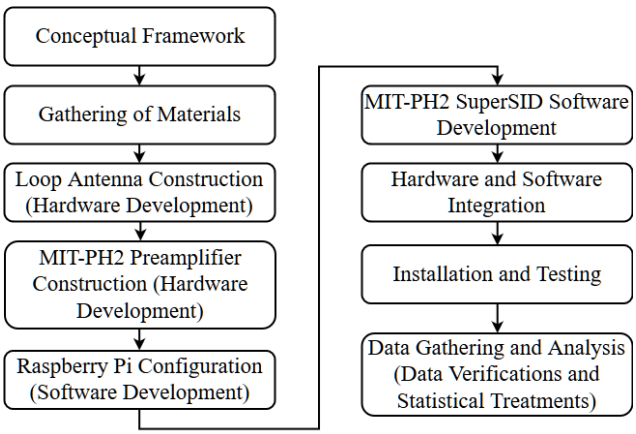

Figure-1. Methodology.

The VLF signal is the sole input for this research while data graphs are the main output for the data acquisition (DAQ) system. The basic process of which the system arrived with a SID data graph is discussed in Figure-2. VLF signals were captured, amplified, and converted to digital signals for further processing by a computing device which runs the SuperSID software.

Figure-2. Conceptual framework.

Hardware development

The study originally opted for a conventional desktop with the SuperSID receiver from Stanford to be treated as true values for the study. Comparing the power spectral density (PSD) and SID data graph using Stanford's SuperSID receiver each for the desktop and the microcomputer setup is illustrated in Figures3 and 4.

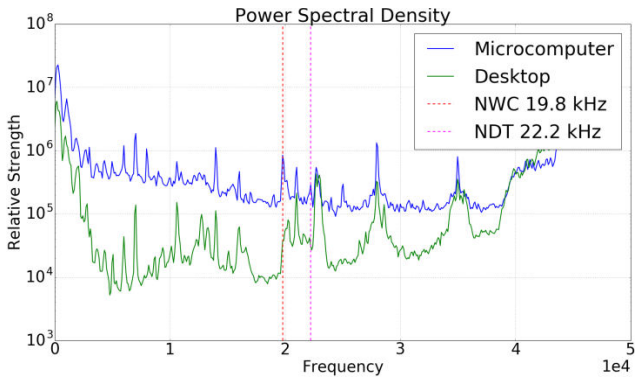

Figure-3. Power spectral density using microcomputer and desktop setup.

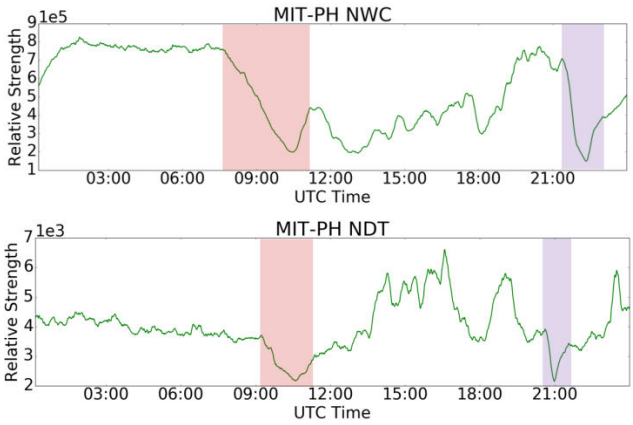

Figure-4a. SID data graphs using raspberry Pi microcomputer setup.

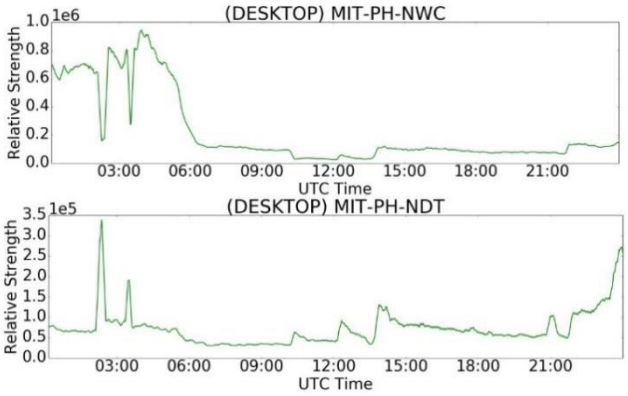

Figure-4b. SID data graphs using desktop setup.

The power spectrum of the microcomputer setup has distinct peaks at the frequencies of desired VLF transmitters unlike the desktop setup. Testing each for SID data graph, the one produced by the microcomputer has distinguishable sunrise and sunset signatures [1]. The red indicator on Figure-4a shows the sunset signature, where the drop in VLF magnitude is observed to be gradual, while the violet indicator shows the sunrise signature, where the drop in magnitude occurred in less time. The areas before the red indicator and after the violet indicator are local daytime in the monitoring station, while the areas in between the indicators are local night time. This figure is also an example of a normal day plot without disturbances, referred to as a quiet day.

Hence, the research setup in Figure-5 was prepared and followed in this research which made use of a Raspberry Pi as the main computing device to run the SuperSID software to produce better results.

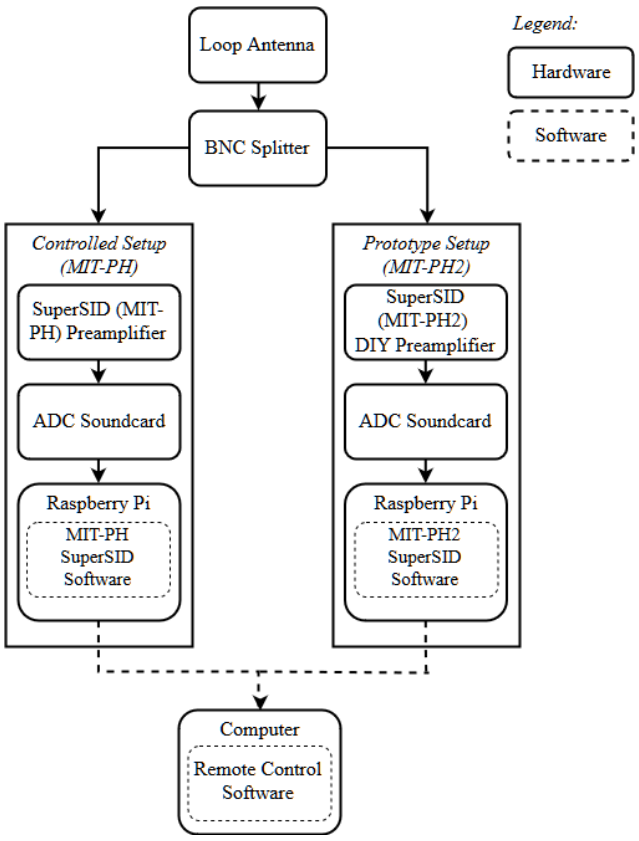

Figure-5. System architecture.

The main components of a DAQ System for monitoring VLF radio signals is illustrated in Figure-6. Radio signals, as acquired through the loop antenna, are split to the two sub-setups using an ordinary tee-connector BNC Splitter. The left-side setup, named MIT-PH, uses Stanford's SuperSID receiver and Eric Gibert's open-source SuperSID software [13]; while the right-side setup or the prototype setup, named MIT-PH2, uses a preamplifier adapted from Stanford SuperSID setup and a modified version of the same open-source SuperSID software. The MIT-PH2 SuperSID preamplifier is redesigned to a single layer PCB which receives a raw input signal from the antenna through the RG-58 coaxial cable. The amplified analog signal is converted to a digital signal using theUSB external soundcard or the ADC, with a sampling rateat 96 kHz, for further processing by the DAQ software. The microcomputer operates without a monitor (headless), however, is administrated remotely to avoid introducing electrical interference or noise to the DAQ system.

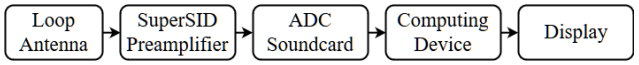

Figure-6. Parts of the DAQ system.

Software development

The Raspbian operating system is installed on both microcomputers. The software makes use of additional libraries aside from the standard python

installation, these libraries include "matplotlib", "wxPython", "numpy" and "alsaaudio" [14].

The following modifications on top of Eric Gibert's SuperSID software were added: (1) a calculation of Quiet Day Curve (QDC), a method acknowledged in different studies, using the mean of quiet days close to the day of interest [15]; (2) a real-time plotting of VLF signal strength for each VLF transmitter mentioned in the software's configuration. The SuperSID software is configured to monitor NWC (19.8 kHz) in Australia and NDT (22.2 kHz) in Japan due to signal reliability and proximity.

Figure-7 shows the daily flow of the modified data acquisition (DAQ) program installed in the microcomputer. The software starts with opening the configuration file that contains the parameters such as the log format and the VLF transmitter stations it is "tuned" into. The microcomputer captures the signal at a defined log interval (5 seconds) and afterwards the power spectrum and the relative strength for each transmitter stations is calculated. The monitored signal strengths for NWC and NDT at that interval is temporarily kept in memory. The signal strength versus time plot for the current day is updated then to the display. The program also logs the hourly raw and filtered signal data.

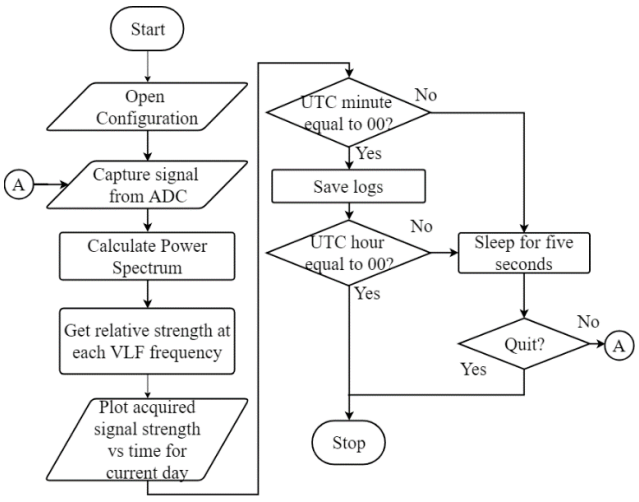

Figure-7. Daily software process.

Installation and testing

After integrating the hardware and software, the microcomputer-based DAQ was tested. The antenna is placed in an area relatively free of electric interference. The preamplifier and Raspberry Pi are located at the nearest secure area with a power source that a coaxial cable connected from the antenna can reach. The whole data acquisition system is situated inside the Mapua University Campus in Manila, Philippines for recording and monitoring data.

For the prototype setup, the "Spectrum" tab similar to Figure-3 displays the power spectrum which is used to determine which VLF signal to monitor. The signal strength of the transmitters with the best peaks were selected and tested for a day to check for diurnal effects (sunrise and sunset signatures). The 'Realtime' tab displays an updating VLF signal strength of the selected transmitter for the current day. An option to plot the QDC together with the real-time plot as illustrated in Figure-8 is added to compare the potential occurrence of disturbances. QDC is calculated automatically from the recent three day data logs at UTC +0 or can be selected from previous data. QDC is produced from the average signal strength (V) of selected quiet days (V_1, V_2, …, V_n) and is defined using Eqn. (1), where n is the number of days selected.

$$V = \frac{1}{n}\sum_1^n V_i \quad (1)$$

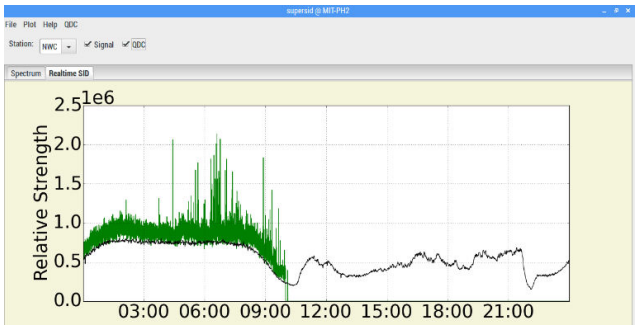

Figure-8. Sample real-time SID data graph comparison with QDC.

DATA GATHERING AND ANALYSIS

It was previously mentioned that SID monitors in the region are lacking, and that the effects of solar flares can be localized. If there is an event in the Sun which has an impact around Asia, it may not be reflected on the SID data graph from other locations. Moreover, observations from different monitor locations and transmitters will manifest different diurnal trends in the data. Therefore, the group obtains data from the controlled setup, MIT-PH, and use it in comparison with MIT-PH2. The acquired data from both setups are assessed using graphical comparison and Pearson Correlation. For graphical comparison, the data graph from the monitors were superimposed with each other as in Figures 9a and 10a. The SID data graph from MIT-PH2 has been observed to have a higher magnitude than that of the MIT-PH, but the trend at which the samples increase, and decrease are similar. Scatter plots in Figures 9b and 10b, suggests a positive linear correlation between the two monitors.

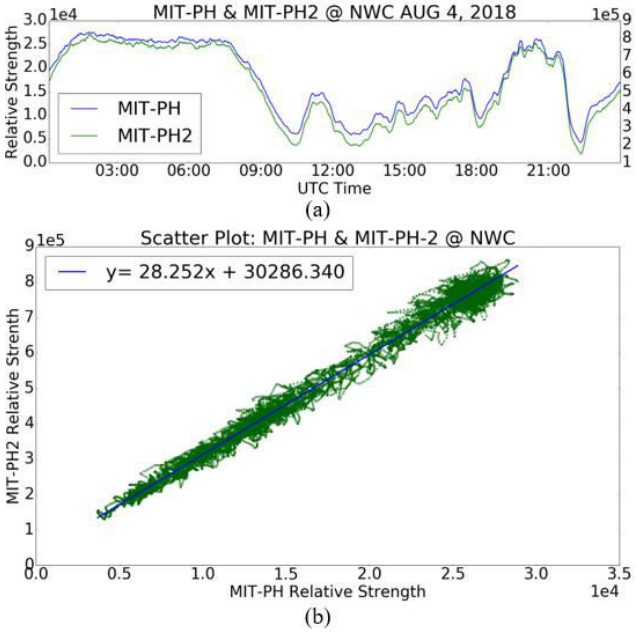

Figure-9.a) Sample graphical comparison of data graphs, and b) Scatter plot diagram between MIT-PH and MIT-PH2 monitoring NWC.

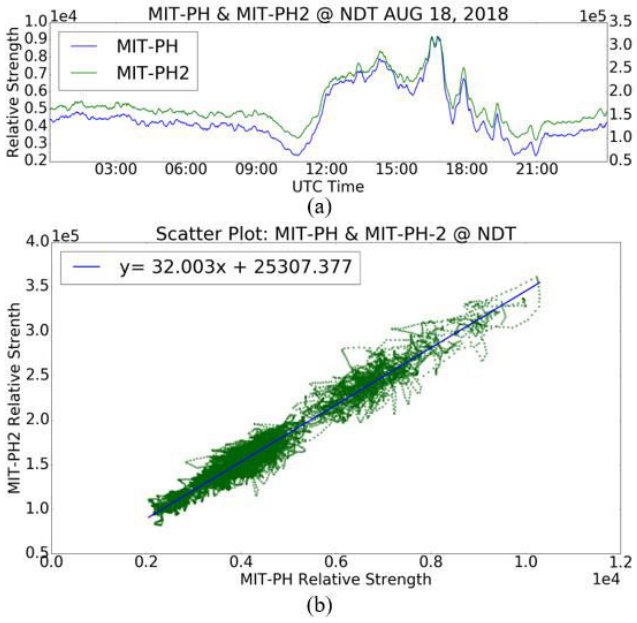

Figure-10.a) Sample graphical comparison of datagraphs, and b) Scatter plot diagram between MIT-PH and MIT-PH2 monitoring NDT.

MIT-PH and MIT-PH2 data are treated using Pearson Correlation which is a statistical test for the strength of association between two datasets [16]. The result of the Pearson correlation coefficient, r, which ranges from –1.0 to +1.0, denotes the strength of association between MIT-PH and MIT-PH2 data. To validate the significance of the relationship between the samples, the P-value of the corresponding correlation is calculated and compared to an alpha value of 0.05.

Figure-11 illustrates the thirty (30) day correlation coefficients between MIT-PH and MIT-PH2 for NWC and NDT transmitters which is averaged to 0.958, and 0.948 respectively. The results are close to a +1.0 value, signifying that there is a positive linear relationship between the two monitors. The calculated P-values are equal to zero which is less than the alpha value therefore implies the correlation is significant [17] and indicates that both are yielding to the same trend and can be used consistently for research purposes.

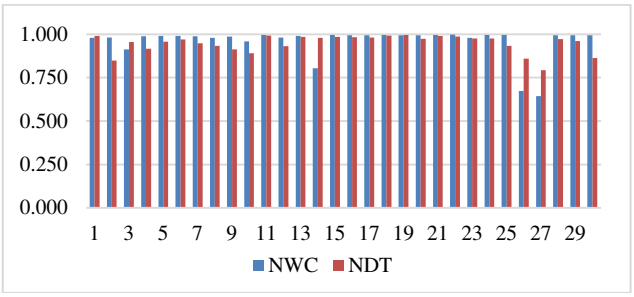

Figure-11. Representation of MIT-PH and MIT-PH2 Correlation for NWC and NDT transmitters.

Verification of disturbances

Disturbances reflect on the SID data graph when there are ionospheric and space weather events. The Geostationary Operational Environmental Satellite (GOES) observe emissions directly from the Sun in space which can be used to validate SIDs but not track the Earth's response to those emissions [5]. For disturbances caused by thunderstorms rainfall tables are utilized from the local meteorological service.

This research used an enhancement algorithm based on a method which distinguishes solar flares from other noises [18]. That algorithm calculates the gradient of each signal received. The analysis covers characterization for sudden ionospheric disturbances based from its signature on the enhanced signal for solar flare and thunderstorm occurrence. The enhancement algorithm is applied to the gathered data from the prototype and from historic SID datasets available at the centralized repository hosted by Stanford. These historic datasets are used to complement the lack of collected prototype data since the study was conducted during minimal solar activity.

In Figure-12, SIDs last September 6, 2017 were observed by AGO (Slovenia) monitor monitoring VLF transmitters GQD (19.6 kHz) and GBZ (22.1 kHz) in the United Kingdom, and ICV (20.27 kHz) in Italy. Every transmitter depicts its own one-day plot. In all the transmitters, signal strengths increased during solar flares events. The peaks in SID data match at times when x-ray flux increases. However, solar flares are "drowned out" during night time [19] and are excluded at local night time as shaded in Figure-12. Information from GOES shows that are seven observed solar flares: two X-class flares (major flares), three M-class flares (moderate flares), and 2 C-class flares (minor flares) (Table-1).

Table-1. Flares for September 6, 2017.

Flare type	Begin (UTC)	Max (UTC)	End (UTC)
C1.6	06:17	06:22	06:29
C2.7	07:29	07:34	07:48
X2.2	08:57	09:10	09:17
X9.3	11:53	12:02	12:10
M2.5	15:51	15:56	16:03
M1.4*	19:21	19:30	19:35
M1.2*	23:33	23:39	23:44

*Solar Flare occurred on the monitoring station's night time

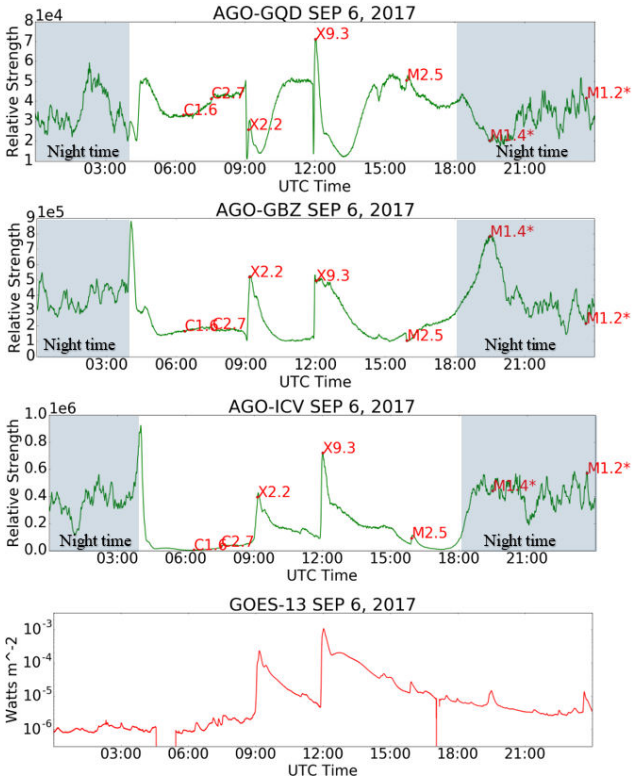

Figure-12. SuperSID plots at three transmitters (GQD, GBZ, and ICV) by AGO and the GOES X-ray flux on September 6, 2017.

Daytime on AGO for September 6, 2017 starts at 3:58 UTC and ends at 18:01 UTC. The enhancement algorithm applied as shown in Figure-13. From the five flares that happened on daytime, only the two X-class flares can be relatively distinguished from the enhanced signals. These flares are characterized by rapid rise and rapid decay in magnitude.

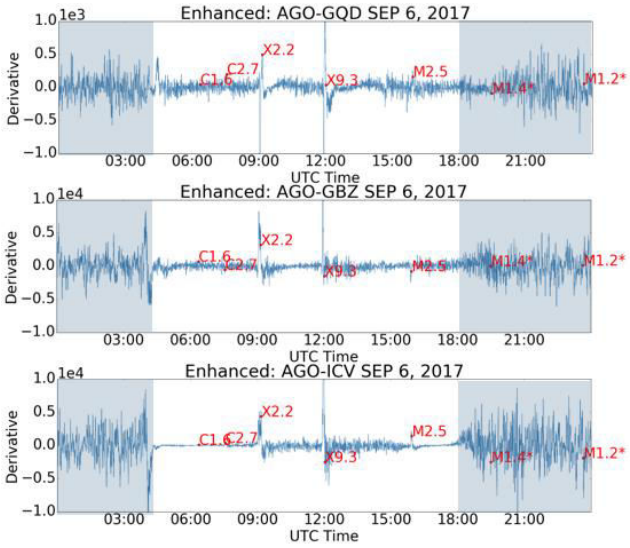

Figure-13. Enhanced signals of chosen VLF transmitters for September 6, 2017.

For a thunderstorm event such as in July 7, 2018, the nearest available 10-minute millimeter rainfall gauge data was used to validate the raw SuperSID data from our prototype, MIT-PH2, as demonstrated on Figure-14. Figure-14b shows a sudden rise in rainfall from 7:20 UTC to 9:40 UTC (15:40 to 17:40 local time). At the same time range, the relative strength of the signal is also disturbed from its usual trend (Figure-13a). Thunderstorm on the enhanced signal can be characterized by vertical lines from both side of the Derivative axis, which implies that there is evident disturbance on the signal over time.

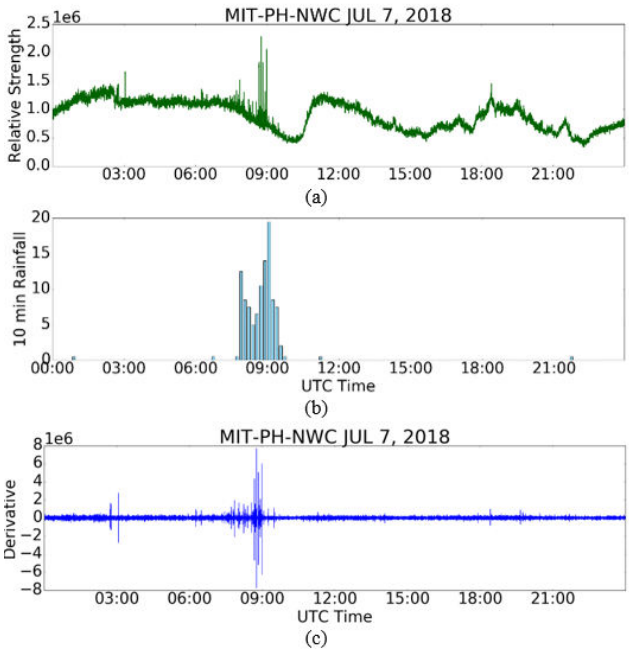

Figure-14. a) Raw SuperSID data observed by MIT-PH2 at NWC, b) 10-minute rainfall data, and c) Enhanced signal for July 7, 2018 UTC.

CONCLUSIONS

A real-time microcomputer-based data acquisition system named MIT-PH2 was developed in this project. MIT-PH2 was able to successfully display real-time signal strength versus time plot for the current day. Also, QDC was plotted together with the real-time plot to compare the potential occurrence of disturbances. It was validated using another SuperSID monitor from Stanford, named MIT-PH. Both are configured to monitor NWC (19.8 kHz) and NDT (22.2 kHz). A statistical test was performed to validate the association between the monitors which resulted with an average correlation coefficient of 0.958 for the dataset from NWC transmitter and 0.948 for NDT transmitter. The correlation coefficient result is close to 1.0 value which indicates that there is a positive linear relationship between the two monitors. Corresponding P-values resulted to zero which implies significant correlation. It can be concluded that both samples are yielding to the same trend and both can be used accurately for research purposes. Also, an enhanced algorithm was applied to the recorded data and from historic SID datasets and was able to successfully characterize solar flare and thunderstorm occurrence. Solar flares on the enhanced signal are characterized by rapid rise and rapid decay in magnitude while a thunderstorm is characterized by vertical lines from both side of the Derivative axis.

ACKNOWLEDGEMENT

The authors would like to express gratitude to Mapua University's Office of Directed Research for Innovation and Value Enhancement for partially funding the materials for this study; to the University's Campus Development and Maintenance Office for giving permission and help to the installation of our antenna; to Stanford University and Society of Amateur Radio Astronomers for granting our request for the SuperSID Monitor; and to Philippine Atmospheric Geophysical and Astronomical Services Administration for the rainfall gauge data.

REFERENCES

[1] Scherrer D. 2007. Research with Space Weather Monitor Data. Stanford, California, USA.

[2] Basu S., Buchau J., Rich F.J. and Weber E.J. 1985. Ionospheric Radio Wave Propagation. In A. Jursa Handbook of Geophysics and the Space Environment. National Technical Information Service. Springfield, Virginia, USA. pp. 10-1-10-3.

[3] Watthanasangmechai K., Yamamoto M., Saito A., Tsugawa T., Yokoyama T., Supnithi P. and Yatini C. Y. 2014. Latitudinal GRBR-TEC estimation in Southeast Asia region based on the two-station method. Radio Science. 49(10): 910-920.

[4] Virginia Geospatial Extension Program. 2013. Chapter 3: Introduction to GPS/GNSS. Blacksburg, Virginia, USA.

[5] Mitchell R., Scherrer D. and Lee S. 2007. SID Users Manual. Stanford, California, USA.

[6] Habarulema J., McKinnella L.A., Buresovac D., Zhangd Y., Seemalae G., Ngwiraf C. and Oppermana B. 2013. A comparative study of TEC response for the African equatorial and mid-latitudes during storm conditions. Journal of Atmospheric and Solar-Terrestrial Physics. 102: 105-114.

[7] Mansilla G.A. 2003. Ionospheric Storm Effects at the Equatorial Anomaly. International Journal of Geomagnetism and Aeronomy. 4(3): 209-214.

[8] Simi K., Manju G., Haridas M.K., Nayar S.R., Pant T.K. and Alex S. 2013. Ionospheric response to a geomagnetic storm during November 8-10, 2004. Earth, Planets and Space. 65(4): 343-350.

[9] Francisca D., Macalalad E., Vallar E., Galvez M.C., Tsai L.-C. and Hsiao T.Y. 2015. VHF/UHF amplitude scintillation observed by the low-latitude ionospheric tomography network (LITN). ARPN Journal of Engineering and Applied Sciences. 10(22): 10324-10327.

[10] Raab F.H., Asbeck P., Cripps S., Kenington P.B., Popovic Z.B., Pothecary N., Sevic J.F. and Sokal N.O. 2002. Power Amplifiers and Transmitters for RF and Microwave. IEEE Transactions on Microwave Theory and Techniques. 50(3): 814-826.

[11] Coat I. 2009. Co-site interference between wideband receiver and switching power supply. In: 2009 Electromagnetic Compatibility Symposium Adelaide. pp. 13-16.

[12] Nwankwo V.U.J. and Chakrabarti S.K. 2013. Effects of Plasma Drag on Low Earth Orbiting due to Heating of Earth's Atmosphere by Coronal Mass Ejections. Cornell University Library.

[13] Gibert, E. 2013. Cross-platform Sudden Ionospheric Disturbances (SID) monitor. GitHub repository. Available (github.com/ericgibert/supersid).

[14] Soon Y., Gan K. and Abdullah M. 2015. Development of Very Low Frequency (VLF) Data Acquisition System Using Raspberry Pi. In: Proceeding of the 2015 International Conference on

Space Science and Communication (IconSpace). Langkawi, Malaysia. 10-12 August 2015. pp. 485-488.

[15] Cresswell-Moorcock K., Rodger C. J., Clilverd M. A. and Milling D. K. 2015. Techniques to determine the quiet day curve for a long period. Radio Science, 50(5): 453-468.

[16] Xie X. and Wang H. 2012. A new method for identifying reliably correlated variables. 2012 9th International Conference on Fuzzy Systems and Knowledge Discovery. pp. 765-769.

[17] Sedgwick P. 2012. Pearson's correlation coefficient. BMJ. doi:10.1136/bmj.e4483.

[18] Mukhtar K. 2014. Sudden Ionospheric Disturbance (SID) Monitor. Available (http://suparco.gov.pk/pages/ presentations-pdf/day-3/session-1/14A-III/4.pdf).

[19] Murray S. 2006. Tracing Particles from the Sun to the Earth's Ionosphere. Available (http://solar-center.stanford.edu/SID/StudentWork/SophieMurray.pdf).